



This discussion paper is/has been under review for the journal Geoscientific Model Development (GMD). Please refer to the corresponding final paper in GMD if available.

Coupling the high complexity land surface model ACASA to the mesoscale model WRF

L. Xu¹, R. D. Pyles², K. T. Paw U², S. H. Chen², and E. Monier¹

¹Joint Program on the Science and Policy of Global Change, Massachusetts Institute of Technology, Cambridge, Massachusetts, USA

²Department of Land, Air, and Water Resources, University of California Davis, Davis, California, USA

Received: 7 February 2014 – Accepted: 28 February 2014 – Published: 5 May 2014

Correspondence to: L. Xu (liyixm@mit.edu)

Published by Copernicus Publications on behalf of the European Geosciences Union.

Title Page

Abstract

Introduction

Conclusions

References

Tables

Figures

◀

▶

◀

▶

Back

Close

Full Screen / Esc

Printer-friendly Version

Interactive Discussion



Abstract

In this study, the Weather Research and Forecasting Model (WRF) is coupled with the Advanced Canopy–Atmosphere–Soil Algorithm (ACASA), a high complexity land surface model. Although WRF is a state-of-the-art regional atmospheric model with high spatial and temporal resolutions, the land surface schemes available in WRF are simple and lack the capability to simulate carbon dioxide, for example, the popular NOAH LSM. ACASA is a complex multilayer land surface model with interactive canopy physiology and full surface hydrological processes. It allows microenvironmental variables such as air and surface temperatures, wind speed, humidity, and carbon dioxide concentration to vary vertically.

Simulations of surface conditions such as air temperature, dew point temperature, and relative humidity from WRF–ACASA and WRF–NOAH are compared with surface observation from over 700 meteorological stations in California. Results show that the increase in complexity in the WRF–ACASA model not only maintains model accuracy, it also properly accounts for the dominant biological and physical processes describing ecosystem-atmosphere interactions that are scientifically valuable. The different complexities of physical and physiological processes in the WRF–ACASA and WRF–NOAH models also highlight the impacts of different land surface and model components on atmospheric and surface conditions.

1 Introduction

Although the Earth is mostly covered by ocean, the presence of land surfaces introduces much complexity into the Earth system that drives numerous atmospheric and oceanic dynamics. The effects of complexity ranges from the simple land–sea contrasts in radiation processes, to the wind flow dynamics, and to the more complex biogeophysical processes of terrestrial systems. Various types of plants, soils, microbes, and all living organisms including humans are situated on and within the landscape

GMDD

7, 2829–2875, 2014

WRF–ACASA coupling

L. Xu et al.

Title Page

Abstract

Introduction

Conclusions

References

Tables

Figures

⏪

⏩

◀

▶

Back

Close

Full Screen / Esc

Printer-friendly Version

Interactive Discussion



WRF–ACASA
coupling

L. Xu et al.

[Title Page](#)[Abstract](#)[Introduction](#)[Conclusions](#)[References](#)[Tables](#)[Figures](#)[◀](#)[▶](#)[◀](#)[▶](#)[Back](#)[Close](#)[Full Screen / Esc](#)[Printer-friendly Version](#)[Interactive Discussion](#)

that make up the Earth's terrestrial system of the biosphere. Though the surface layer represents a very small fraction of the planet, only the lowest 10% of the planetary boundary layer, it has been widely regarded as a crucial component of the climate system (Stull, 1988; Mintz, 1981; Rowntree, 1991). The interaction between the land surface (biosphere) and the atmosphere is therefore one of the most active and important aspects of the natural system.

Vegetation on land surfaces introduces complex structures, properties, and interactions. Therefore, vegetation heavily modifies surface exchanges of energy, gas, moisture, and momentum in ways that develop the microenvironment, distinguishing vegetated surfaces from landscapes without vegetation. Such influences are known to occur on different spatial and temporal scales (Chen and Avissar, 1994; Pielke et al., 2002; Zhao et al., 2001). In particular, often near-geostrophically-balanced wind patterns are disrupted in the lower atmosphere when wind encounters vegetated surfaces i.e., the winds slow down and change direction as a result of turbulent flows that develop within and near the vegetated canopies (Wieringa, 1986; Pyles et al., 2004).

Depending in part on the canopy height and structure, wind and turbulent flows often vary considerably across different ecosystems—even when each is presented with the same meteorological and astronomical conditions aloft. Gradients in heating, air pressure, and other forcings develop across heterogeneous landscapes, helping to sustain atmospheric motion. Hence, since the surface layer is the only physical boundary in an atmospheric model, there is a consensus that accurate simulations of atmosphere processes in an atmospheric model require good representations of the surface layer and its terrestrial system. Models that account for the effects of surface layer on climate and atmosphere conditions are referred to as the Land Surface Models (LSMs).

Unfortunately, the current land surface models, i.e., the widely used set of four schemes present in the Weather Research and Forecasting (WRF) model (5-layer thermal diffusion, Pleim-Xiu, Rapid Update Cycle, and the popular NOAH, often overly simplify the surface layer by using a single layer “big leaf” parameterizations and other assumptions, usually based around some form of bulk Monin–Obukhov-type similarity

theory (Chen and Dudhia, 2001a, b; Pleim and Xiu, 1995; Smirnova et al., 1997, 2000; Xiu and Pleim, 2001). These models scale the leaf-level physical and physiological properties as one extensive “big leaf” to represent the entire canopy.

The majority of the land surface models do not simulate carbon dioxide flux, even as it is largely recognized as a major contributor to the current climate change phenomenon and a controller of plant physiology. Plant transpiration in these models is often based on the Jarvis parameterization, in which the stomatal control of transpiration is a multiplicative function of meteorological variables such as temperature, humidity, and radiation (Jarvis, 1976). However, a large number of studies show that there is a strong linkage between the physiological process of photosynthetic uptake and respiratory release of CO₂ to plant transpiration through stomata (Zhan and Kustas, 2001; Houborg and Soegaard, 2004). Hence, physiological processes related to CO₂ exchange rates should be included in surface-layer representation of water and energy exchanges.

Oversimplification of surface processes and their impacts on the atmosphere in these land surface models are likely to misrepresent and poorly predict surface and atmosphere interactions. Such models in Earth science fields that use simplified equations and statistical relationships to represent complex processes in physics, physiology, hydrology, and thermodynamics require intense fine-tuning and optimization algorithms to match the observations (Duan et al., 1992). These empirical models are capable of producing good results, but their assumptions limit their ability to investigate relationship and feedbacks between different components of the system. For example, the empirical models are unable to characterize the relationship between canopy height and their sub-canopy energy distribution, and the effects of increased carbon dioxide concentrations on vegetation–atmosphere interactions. This is especially true for regional scale studies where the influence of the terrestrial system increases with better spatial resolution and heterogeneous land cover.

Recent computer and model developments have greatly improved atmospheric modeling abilities. Progressively more complex planetary boundary layer and surface

**WRF–ACASA
coupling**

L. Xu et al.

Title Page

Abstract

Introduction

Conclusions

References

Tables

Figures

◀

▶

◀

▶

Back

Close

Full Screen / Esc

Printer-friendly Version

Interactive Discussion



WRF–ACASA coupling

L. Xu et al.

Title Page

Abstract

Introduction

Conclusions

References

Tables

Figures

◀

▶

◀

▶

Back

Close

Full Screen / Esc

Printer-friendly Version

Interactive Discussion



schemes are being implemented into these atmosphere models with higher spatial and temporal resolution. However, the challenges involved in advancing the robustness of land surface models continue to limit the realistic simulation of planetary boundary layer forcing by vegetation, topography, and soil. Some have argued that the increase in model complexity does not translate into higher accuracy due to the increase in uncertainty introduced by the large number of input parameters needed by the more process-based models (Raupach and Finnigan, 1988; Jetten et al., 1999; de Wit, 1999; Perrin et al., 2001). However, there is a certain scientific value in properly accounting for the dominant biological and physical processes describing ecosystem-atmosphere interactions, even if this greatly complicates the models.

This study introduces the novel coupling of the mesoscale WRF model with the complex multilayer Advance Canopy–Atmosphere–Soil Algorithm (ACASA) model, to improve the surface and atmospheric representation in a regional context. The objectives of this study are to (1) parameterize complex land surface processes that drive local mesoscale circulations, and (2) to investigate the effects of model complexity on accuracy.

2 Models, methodology and data

2.1 The Weather Research and Forecasting (WRF) model

The mesoscale model used in this study is the Advanced Research WRF (ARW) model Version 3.1. WRF is a state-of-the-art, mesoscale numerical weather prediction and atmospheric research model developed by a collaborative effort of the National Center for Atmospheric Research (NCAR), the National Oceanic and Atmospheric Administration (NOAA), the Earth System Research Laboratory (ESRL), and many other agencies. The WRF model contains a nearly complete set of compressible and non-hydrostatic equations for atmospheric physics (Chen and Dudhia, 2000). Multiple atmospheric layers vary in vertical grid spacing with height to simulate three-dimensional atmospheric

**WRF–ACASA
coupling**

L. Xu et al.

[Title Page](#)[Abstract](#)[Introduction](#)[Conclusions](#)[References](#)[Tables](#)[Figures](#)[◀](#)[▶](#)[◀](#)[▶](#)[Back](#)[Close](#)[Full Screen / Esc](#)[Printer-friendly Version](#)[Interactive Discussion](#)

variables. The mass-based terrain following coordinate in WRF improves the surface processes. It is commonly used to study air quality, precipitation, severe windstorm events, weather forecasts, and many other atmospheric related conditions (Borge et al., 2008; Thompson et al., 2004; Powers, 2007; Miglietta and Rotunno, 2005; Trenberth and Shea, 2006). Compared to the 2.5° (equivalent to 250 km^2) resolution of General Circulation Models (GCMs), the WRF model with high spatial and temporal resolution is more suitable to study climate conditions over California; WRF can be nested so that fine grid spacing of on the order of 1 km or less is possible.

Four different parameterizations of land-surface processes are available in the WRF model as mentioned in the introduction. WRF's more widely used and most sophisticated NOAH employs simplistic physics compared to ACASA, being more akin to the set of ecophysiological schemes that include SiB and BATS (Dickinson et al., 1993; Sellers et al., 1996). There is only one vegetated surface layer in the NOAH scheme, along with four soil layers to calculate soil temperature and moisture. The “big leaf” approach assumes the entire canopy has similar physical and physiological properties to a single big leaf. Energy and mass transfers for the surface layer are calculated using simple surface physics (Noilhan and Planton, 1989; Holtslag and Ek, 1996; Chen and Dudhia, 2000). For example, the surface skin temperature is linearly extrapolated from a single surface energy balance equation, which represents the combined surface layer of ground and vegetation (Mahrt and Ek, 1984). Surface evaporation is computed using modified diurnally dependent Penman–Monteith equation from Mahrt and Ek (1984) and the Jarvis parameterization (Jarvis, 1976). The current WRF LSMs are relatively simple, when compared to the higher order closure based ACASA model, and none of them calculate carbon flux. Hence, there is good justification for use of a fully coupled WRF–ACASA model, which can handle carbon dioxide fluxes and the reaction of ecosystems to increased carbon dioxide concentrations.

2.2 The Advanced Canopy-Atmosphere-Soil Algorithm (ACASA) model

Compared to the simple NOAH, the ACASA model version 2.0 is a complex multilayer analytical land surface model, which simulates the microenvironment profiles and turbulent exchange of energy, mass, CO₂ and momentum within and above ecosystems that constitute land surfaces. It represents the interaction between vegetation, soil and the atmosphere based on physical and biological processes described from the scale of leaves (microscale), and horizontal scales on the order of 100 times the ecosystem vegetation height, i.e., hundreds of meters to around 1 km. The surface layer is represented as a column model with multiple vertical layers extending to the lowest planetary boundary. The model has 10 vertical atmospheric layers above-canopy, 10 intra-canopy layers, and 4 soil layers.

For each canopy layer, leaves are oriented in 9 sun-lit angle leaf classes (random spherical orientation) and 1 shaded leaf class in order to represent radiation transfer and leaf temperatures in a representative and variable array that aggregates to simulate realistic exchanges for sensible heat, water vapor, momentum, and carbon dioxide. The values of fluxes at each layer depend on those from all layers, so the longwave radiative and turbulence equations are iterated until numerical equilibrium is reached. Shortwave radiation fluxes, along with associated arrays (probabilities of transmission, beam extinction coefficients, etc.), are not changed while the other sets of equations are iterated to numerical convergence.

Plant physiological processes, such as evapotranspiration, photosynthesis and respiration, are calculated for each of the leaf classes and layers, based on the simulated radiation field and the micrometeorological variables calculated in the previous iteration step. The default maximum rate of Rubisco carboxylase activity, which controls plant physiological processes is provided for each of the standardized vegetation types, although specific values of these parameters can be entered. Temperature, mean wind speed, carbon dioxide concentration, and specific humidity are calculated explicitly for

GMDD

7, 2829–2875, 2014

WRF-ACASA coupling

L. Xu et al.

Title Page

Abstract

Introduction

Conclusions

References

Tables

Figures

◀

▶

◀

▶

Back

Close

Full Screen / Esc

Printer-friendly Version

Interactive Discussion



each layer, using the higher order closure equations (Meyers and Paw U, 1986, 1987; Su et al., 1996).

In addition to the capability to calculate the carbon dioxide flux, a key advanced component of the ACASA model is its higher-order turbulent closure scheme. The parameterizations of the fourth-order terms used to solve the prognostic third order equations are described by assuming a quasi-Gaussian probability distribution as a function of second-moment terms (Meyers and Paw U, 1987). Compared to lower order closure models, the higher order closure scheme increases the model accuracy through improving the description of the turbulent transport of energy, momentum, and water by both small and large eddies. While in small-eddy theory or eddy viscosity, energy fluxes move down a local gradient, large eddies in the real atmosphere can transport flux against the local gradient. Such counter-gradient flow is a physical property of large eddies associated long distance transport. For example, mid-afternoon intermittent ejection-sweep eddies that cycle deep into a warm forest canopy with snow on the ground, from regions where air temperatures could have values between that of the warm canopy and the cold snow surface, would result in overturning of eddies to transport relative warm air from above the canopy through the canopy to the snow surface below. The local gradient from the canopy to the above-canopy air would incorrectly indicate sensible heat going upwards, instead of the actual heat flow down to the snow past the canopy due to the long turbulence scales of transport. These potentially counter-gradient transports are responsible for much of land surface evaporation, heat, carbon dioxide and momentum fluxes (Denmead and Bradley, 1985; Gao et al., 1989). The ACASA model uses higher order closure transport between multiple layers of the canopy, mimicking non-local transport, allowing the simulation of counter-gradient and non-gradient exchange. However, with only one surface layer, the simple lower order turbulent closure model NOAH is limited to only down-gradient transport and not mixing within the canopy.

Both rain and snow forms of precipitation are intercepted by the canopy elements in each layer. Some of the precipitation is retained on the leaf surfaces to modify the

WRF–ACASA
coupling

L. Xu et al.

Title Page

Abstract

Introduction

Conclusions

References

Tables

Figures

◀

▶

◀

▶

Back

Close

Full Screen / Esc

Printer-friendly Version

Interactive Discussion



WRF–ACASA coupling

L. Xu et al.

Title Page

Abstract

Introduction

Conclusions

References

Tables

Figures

◀

▶

◀

▶

Back

Close

Full Screen / Esc

Printer-friendly Version

Interactive Discussion



microenvironment of the layers for the next time step, depending on the precipitation amount, canopy storage capacity, and vaporization or sublimation rate. The remaining precipitation is distributed to the ground surface, influencing soil moisture and/or surface runoff as calculated by the layered soil model. The soil model physics in ACASA are very similar to the diffusion physics set used in Noah, but with enhanced layering of the snowpack for more representative thermal profiles throughout deep snow. The multilayer snow model allows interactions between layers and more effectively calculate energy distribution and snow hydrological processes such as snow melt when surface snow experiences higher or lower temperatures than the underlying snow layers. This is important over regions with high snow depth such as Sierra Nevada Mountain where snow is an important source of water. The multilayer snow hydrology scheme has been well tested during the SNOWMIP project (Etchevers et al., 2004; Rutter et al., 2009), where ACASA performed as well or better than many snow models by accurately estimating the snow accumulation rate as well as the timing of the snow melt in a wide range of biomes.

The stand-alone version of the ACASA model has been successfully applied to study sites across different countries, climate systems, and vegetation types. These include a 500 year old growth coniferous forest at the Wind River Canopy Crane Research Facility in Washington State (Pyles et al., 2000, 2004), a spruce forest in in the Fichtelgebirge Mountains in Germany (Staudt et al., 2011), and a maquis ecosystem in Sardinia near Alghero (Marras et al., 2008), and a grape vineyard in Tuscany near Montelcino, Italy (Marras et al., 2011).

2.3 The WRF–ACASA coupling

In an effort to improve the parameterization of land surface processes and their feedbacks with the atmosphere, ACASA is coupled to the mesoscale model WRF as a new land surface scheme. The schematic diagram of Fig. 1 represents the coupling between the two models. From the Planetary Boundary Layer (PBL) and above, the WRF model provides meteorological variables as input forcing to the ACASA land surface model at

**WRF–ACASA
coupling**

L. Xu et al.

[Title Page](#)[Abstract](#)[Introduction](#)[Conclusions](#)[References](#)[Tables](#)[Figures](#)[◀](#)[▶](#)[◀](#)[▶](#)[Back](#)[Close](#)[Full Screen / Esc](#)[Printer-friendly Version](#)[Interactive Discussion](#)

the lowest WRF sigma-layer. These variables include solar shortwave and terrestrial (atmospheric thermal long-wave) radiation, precipitation, humidity, wind speed, carbon dioxide concentration, and barometric pressure. Radiation is partitioned into thermal IR, visible (PAR) and NIR by the ACASA model, which treats these radiation streams separately owing to the preferential scattering of the different wavelengths by vegetation as the radiation passes through the canopy. Part of the radiation is reflected back to the PBL according to the layered canopy radiative transfer model, with the remaining radiation driving the canopy energy balance components and photosynthesis.

Differing from the single layer NOAH surface model coupled to WRF, ACASA creates a normalized vertical LAI or LAD (Leaf Area Density) for the multiple canopy layers according to vegetation type. This is crucial because the canopy height and distribution of LAD have direct influences over the interactions of wind, light, temperature, radiation, and carbon between the atmosphere and the surface layer.

2.4 Model setup

The WRF model requires input data for prognostic variables including wind, temperature, moisture, radiation, and soil temperature, both for an initialized field of variables through the domain, and at the boundaries of the domain. In this study, these input data are provided by the Northern America Regional Reanalysis (NARR) dataset to drive the WRF–NOAH and WRF–ACASA models. Unlike many other reanalysis data sets with coarse spatial resolution such as ERA40 (European Center for Medium-Range Weather Forecasts 40 Year Re-analysis) and GFS (Global Forecast System), NARR is a regional data set specifically developed for the Northern American region. The temporal and spatial resolutions of this data set are 3 h and 32 km, respectively.

Simulations of both the default WRF–NOAH and the WRF–ACASA models were performed for two yearly simulations (2005 and 2006) with horizontal grid spacing of 8 km × 8 km. These two years were chosen because they provide the most extensive set of surface observation data. The model domain covers all of California with parts of neighboring states and the Pacific Ocean to the west, shown in Fig. 2. The complex

WRF–ACASA
coupling

L. Xu et al.

[Title Page](#)[Abstract](#)[Introduction](#)[Conclusions](#)[References](#)[Tables](#)[Figures](#)[◀](#)[▶](#)[◀](#)[▶](#)[Back](#)[Close](#)[Full Screen / Esc](#)[Printer-friendly Version](#)[Interactive Discussion](#)

terrain, and vast ecological and climatic systems in the region make it ideal to test the WRF–NOAH and WRF–ACASA coupled model performances. The geological and ecological regions extend eastward from the coastal range shrub lands to the Central Valley grasslands and croplands, then to the foothill woodlands before finishing at the coniferous forests along the Sierra Nevada range. Further inland to the east and south includes the Great Basin and Range Chaos, an arid and complex mosaic of forests and chaparral tessellated amid the myriad fossae that erupt between dunes and playas. The contrasting moist Northern and semiarid Southern California landscapes are also represented in tandem.

Beside the differences in the land surface model, both WRF–NOAH and WRF–ACASA employ the same set of atmosphere physics schemes stemming from the WRF model. These include the Purdue Lin et al. scheme for microphysics (Chen and Sun, 2002), the Rapid Radiative Transfer Model for long wave radiation (Mlawer et al., 1997), Dudhia scheme for shortwave radiation (Dudhia, 1989), Monin–Obukhov Similarity scheme for surface layer physics of non-vegetated surfaces and the ocean, and the MRF scheme for the planetary boundary layer (Hong and Pan, 1996). WRF runs its atmospheric processes at a 60 s time step, while the radiation scheme and the land surface schemes are called every 30 min. Because ACASA assumes quasi-steady-state turbulent processes, its physics are not considered advisable for shorter time intervals. Both NOAH and ACASA calculate surface processes and update the radiation balance, as well as heat, water vapor, and carbon fluxes, surface temperature, snow water equivalent, and other surface variables in WRF. Analytical nudging of four dimensional data assimilation (FDDA) is applied to the atmosphere for all model simulations in order to maintain the large-scale consistency and reduce drifting of model simulation from the driving field over time. Such nudging (FDDA) is commonly practiced in limited-area modeling and current methods active in WRF are widely accepted through rigorous testing (Stauffer and Seaman, 1990; Stauffer et al., 1991).

2.5 Data

The main independent observational datasets used to evaluate the model simulations were obtained from the Meteorological Section of the California Air Resource Board (ARB). The NARR data were not used for the evaluation as the dataset is used for FDDA during both model simulations. The ARB meteorology dataset comprises over 2000 surface observation stations in California from multiple agencies and programs: Remote Automated Weather Stations (RAWS) from the National Interagency Fire Center, the California Irrigation Management Information System (CIMIS), National Oceanic and Atmospheric Administration (NOAA), Aerometric Information Retrieval System (AIRS), and the Federal Aviation Administration. Potential measurement error and uncertainties are expected in the ARB data because of the differences in station setups and measurement guidelines from the different agencies. For example, ambient surface air temperature is measured at various heights between 1 to 10 m above the ground, depending on the measuring agency. Some stations are located in urban environments, while the model simulations are focused on natural vegetated environments. Therefore, some bias between the observation and simulation over densely populated area is likely. However, with hourly data from over 2000 observation stations within the study domain, the ARB dataset is valuable. Out of the 2000 surface stations in the overall current ARB database, there were about 730 stations operational during the study period of 2005 and 2006 (Fig. 3).

The meteorological and surface conditions from the WRF–NOAH and WRF–ACASA model simulations were evaluated using the Air Resource Board data both for the regional scale level performance, and for specific stations for more in-depth analysis. This represents in no uncertain terms the most rigorous test of ACASA to date, in terms of the sheer number of ACASA point-simulations and the number of ACASA points linked in both space and time. This investigation is therefore represents a significant elaboration upon earlier work (Pyles et al., 2003). Meteorological variables such as surface air temperature, dew point temperature, and precipitation from the two model

GMDD

7, 2829–2875, 2014

WRF–ACASA coupling

L. Xu et al.

Title Page

Abstract

Introduction

Conclusions

References

Tables

Figures

◀

▶

◀

▶

Back

Close

Full Screen / Esc

Printer-friendly Version

Interactive Discussion



WRF–ACASA
coupling

L. Xu et al.

[Title Page](#)[Abstract](#)[Introduction](#)[Conclusions](#)[References](#)[Tables](#)[Figures](#)[◀](#)[▶](#)[◀](#)[▶](#)[Back](#)[Close](#)[Full Screen / Esc](#)[Printer-friendly Version](#)[Interactive Discussion](#)

that of the simulation grid point. Many stations are within patches of specific landscape types that may differ significantly from the overall grid point landscape. Even more challenging is the fact that the WRF–ACASA simulations have outputs for the temperatures within a canopy, so for orchards or forests, the 2 m height (surface) simulation data are not expected to match the 2 m height observations well. WRF–ACASA simulations at 2 m height for the taller plant ecosystems represents temperatures within the plant canopy or in the understory; yet the observations from the ARB network are never in such locations, but rather they are over other surfaces not representative of the simulation grid-point, and usually not even at the 2 m height. The WRF–NOAH simulations do not suffer the same problems compared to the observations in terms of the 2 m height falling in the understory, because the NOAH surface model is a big-leaf model, so the 2 m height represents a height more similar in characteristics to the observations. Despite these significant shortcomings, to maximize the number of observations, the ARB data were chosen because of the large number of stations throughout the simulation domain. The results from year 2005 and year 2006 are similar, so only year 2006 is presented here.

3 Results and discussion

The monthly mean temperatures near the surface over California from both model simulations are compared against the surface observations in Fig. 5. The left panel shows the ARB data (gathered at approximately 10 m above the ground), where the white areas represent regions with missing observations. The WRF–NOAH and WRF–ACASA simulation outputs are represented in the center and right hand panels. The region's geographical complexity is highlighted by the spatial and temporal variations in the surface temperature. The warm summer and cool winter are typical of a Mediterranean-type climate. In addition to the seasonal variation, both WRF–ACASA and WRF–NOAH models are able to capture the distinct characteristics of the warm Central Valley and semiarid region of Southern California. The large flat Central Valley is dominated by

Irrigated Cropland and Pasture, and surrounded by Cropland/Grassland Mosaic. The cold temperatures over the mountain regions are also visible from the surface temperature field. However, there are noticeable differences between the WRF–ACASA and the WRF–NOAH over the Central Valley.

During the month of February, there is a distinct feature of a colder Central Valley surrounded by a slightly warmer region in the WRF–ACASA output. A similar effect is also visible in the month of November, when WRF–ACASA experiences a cold bias over the Central Valley. The temperature contrast of this region is mostly due to the differences in land cover type as well as leaf area index associated with the land cover (Fig. 2). These two variables control important plant physiological processes in the WRF–ACASA model such as photosynthesis, respiration, and evapotranspiration. Lower plant leaf area index for the area surrounding Central Valley leads to less transpiration than in higher LAI Central Valley areas, which has higher partitioning of available energy to latent heat and less to sensible heat.

While the WRF–ACASA model is highly influenced by vegetation cover and the changes in LAI, the surface processes in WRF–NOAH rely heavily on the prescribed minimum canopy resistance for each of the vegetation type. Therefore, the contrast in temperature on over regions of different vegetation cover and leaf area index is more pronounced in the WRF–ACASA model than the WRF–NOAH model. The overall agreement between the model simulations from WRF–ACASA and WRF–NOAH agree well with the surface observation throughout the year. However, the WRF–ACASA experiences a cold bias over the high LAI region in the Central Valley during the month of August. Once again it should be noted that the WRF–ACASA output and the observations are generally not at the same height as the observation height, and the local vegetation type commonly differs from that surrounding the observation sites. The high complexity WRF–ACASA relies on the leaf area index to simulate plant physiological processes and energy budget. High LAI values implicit in the Central Valley land use types within ACASA, when compared to the lower values of remotely sensed LAI during the summer months could result in overestimated of evapotranspiration over the region

**WRF–ACASA
coupling**

L. Xu et al.

Title Page

Abstract

Introduction

Conclusions

References

Tables

Figures

◀

▶

◀

▶

Back

Close

Full Screen / Esc

Printer-friendly Version

Interactive Discussion



as seen in the Central Valley bias. The WRF–NOAH model is less sensitive because it uses prescribed canopy resistances. This highlights the conundrum of advancing model physics—more sophisticated models become more exposed to input data quality as they become more representative of variations in land use type.

5 Figure 6 shows time series of surface air temperature simulated by WRF–ACASA and WRF–NOAH and observations at four different stations for the months of February, May, August, and November 2006. It shows that both WRF–ACASA and WRF–NOAH perform well in simulating the temporal pattern of temperature changes across the seasons and stations (four stations representing the Northeast Plateau Station, the Mojave Desert Station, San Joaquin Valley station, and the Mountain Counties Station). Even short time weather events are clearly detectable in the simulated temperature changes. One such example is the Northeast Plateau station during the month of November, when it experienced with a 20 °C plunge in temperature followed by a warming of 10 °C within five days. Both models are able to simulate this short time weather event.

10 There are differences between the WRF–ACASA and WRF–NOAH performances by time and location. While the model simulations from both models agree well with the surface observation during the cold season of February and November, they differed during the warmer months. During the month of May over the Mojave Desert station, the WRF–ACASA model started with good agreement with the surface observation but gradually differed with time. The daily minimums (or nighttime temperatures) during the month became cooler than the surface observation with time. During August, the nighttime temperatures were consistently 3 to 4 °C cooler than the observed nighttime temperature. PBL heights at night using both NOAH and ACASA were the same as in minimum sigma-layer heights in WRF. This may be excessively shallow given observations suggesting nocturnal PBL heights over deserts to be on the order of 100 to 300 m (Stull, 1988). ACASA results for nighttime cooling would be influenced to a cold bias if the PBL were too shallow, as the negative sensible heat flux would become “trapped” in the shallow inversion layer. ACASA is potentially more sensitive to this than NOAH

**WRF–ACASA
coupling**

L. Xu et al.

Title Page

Abstract

Introduction

Conclusions

References

Tables

Figures

◀

▶

◀

▶

Back

Close

Full Screen / Esc

Printer-friendly Version

Interactive Discussion



The daytime temperatures of WRF–NOAH exceed the observed temperature range over San Joaquin Valley Station.

Further investigation into the temperature differences between the two models in time evolution and diurnal pattern reveals that these are results of differences in model representations of land cover type as well as canopy structure of the two models. Both models agree the best with the observation over the Northeast Plateau station. The site information indicated that this station is located over short vegetated grassland, which matches the land cover type assigned by the WRF model to that particular 8 km × 8 km grid-point. Even though the WRF–ACASA model uses a multilayer canopy representation for all its land cover types, there is no significant difference between the two models over this simple short grass canopy regardless the number of layers. However as the canopy become taller and more complex, the representations of canopy structure and plant physiology become more important. Most importantly, the correct representation of land cover is crucial. For example, the WRF model assigns a vegetation type of Evergreen Needleleaf Forest to the 8 km × 8 km grid point of the Mountain County Station. However, a closer look at the MC station shows that the station is actually located at the edge of the forest over a large clear-cut short grass area instead of within the forest as assumed by the WRF–ACASA model, and above a single big leaf rough surface by the WRF–NOAH model. This mismatch of land cover type seems to be more problematic to the WRF–ACASA model than the WRF–NOAH model in its temperature simulations, probably because the single-leaf NOAH description is closer to a short grass area for observed air temperatures at this site, than temperatures in the understory of a forest as in ACASA.

While a single layer land surface model is used in the WRF–NOAH, the WRF–ACASA assumes a 17 m canopy height with 10 vertical layers for this vegetation type. The surface air temperature simulated by the WRF–ACASA’s multilayer canopy structure and its radiation transfer scheme is therefore a surface air temperature within the canopy with overhead shading from tall trees, and with the microclimatic influences of understory temperature and humidity. Due to less direct heating from shortwave

WRF–ACASA
coupling

L. Xu et al.

Title Page

Abstract

Introduction

Conclusions

References

Tables

Figures

◀

▶

◀

▶

Back

Close

Full Screen / Esc

Printer-friendly Version

Interactive Discussion



WRF–ACASA
coupling

L. Xu et al.

[Title Page](#)[Abstract](#)[Introduction](#)[Conclusions](#)[References](#)[Tables](#)[Figures](#)[◀](#)[▶](#)[◀](#)[▶](#)[Back](#)[Close](#)[Full Screen / Esc](#)[Printer-friendly Version](#)[Interactive Discussion](#)

radiation, the daytime temperatures within the canopy layers as simulated by the WRF–ACASA model during the warm seasons of May and August are respectively lower than the surface air temperature measured over a short grass area near the forest. In addition, the Needleleaf forest land cover type used in the WRF–ACASA model experiences turbulent transport and mixing of energy, moisture, gas, and momentum within the canopy layers as results from the higher-order turbulent closure scheme. Therefore, unlike environmental conditions at the station at 2 m height above the short grass area, the air at 2 m height within the WRF–ACASA tall canopy experiences a drastic reduction in nighttime heat loss. Hence, the surface air temperatures of the WRF–ACASA simulation are higher than the surface observation during the nights of February and November. Such details of canopy structures and their associated thermodynamic processes, however, are lacking from the single layer WRF–NOAH model, and do not match the observational site characteristics.

As mentioned before, the WRF–ACASA model tends to underpredict temperature observations during early summer morning in the Mojave Desert and the WRF–NOAH model tends to overpredict temperature all day. The prolonged cooling in the morning simulated by the WRF–ACASA model is associated with the low vegetated cover over shrublands. In this situation, more energy is lost from the surface to the atmosphere. In general, the model performances from WRF–ACASA and WRF–NOAH vary depending on the season and the vegetation cover. The cool biases seen in desert regions may also be due to the nocturnal inversion issue described earlier.

Figure 8 shows scatter plots of simulated monthly surface air temperature from the WRF–ACASA and WRF–NOAH model vs. observations sorted by seasons for the four basins defined previously. Each of the points represents a monthly average for one station in the specified basin, and the colors indicate seasons. Least squares regression of the seasonal data shows that both model simulations approach a 1 : 1 line relationship with the observations. There are some small differences in performances between the two models depending on seasons and locations. This collective analysis of all stations

from the four basins shows that although there are some cold biases over the Mojave Desert station the models perform well across the entire basin.

Table 2 and Fig. 9 present the statistical analysis of the WRF–ACASA and WRF–NOAH near-surface temperature outputs for each of California’s 13 basins. Statistical values of R -square value, Root Mean Square Error (RMSE), and Degree of Agreement are calculated for each of the basin for each of four seasons. The Coefficient of Determination or (R -square) represents the correlation of the model simulation with the surface observation. The RMSE shows the relative errors of the model simulation against the observation, while the Degree of Agreement is a statistical method to assess the agreement between the model simulations with the surface observation.

Overall, both of the models have a high degree of agreement with all 700 observation stations within the 13 ARB basins during Winter, Spring, and Autumn. The dry summer season is more problematic than the other seasons for both of the models and more so for the WRF–ACASA model over coastal regions such as South Coast, San Diego, and San Francisco basins. This is most noticeable in the RMSE values for WRF–ACASA over the low vegetated regions of Great Basin Valley (GBV), Salton Sea (SS), and San Diego (SD), which increased dramatically during the warm season. While the degree of agreement for the San Francisco Basin (SFB) during the wintertime is high with values above 0.8 for both models, the R -square values show that there is little correlation between the model simulations and the surface observations. It could be due to the small range of observation data. Overall, the temperature simulations from both models agree well with the observations where the degree of agreement is high. Previous examination on a station-by-station basis also reveals that there is a mismatch in vegetation cover between the WRF models and the actual surface station, such as the Mountain Counties station. These mismatches introduce errors that are not due to model physics, and they contribute to some of the low R -square and high RMSE values in the collective study.

Figure 10 shows time series of surface dew point temperature over the same four stations. The dew point temperature is another important variable that influences the

WRF–ACASA coupling

L. Xu et al.

Title Page

Abstract

Introduction

Conclusions

References

Tables

Figures

◀

▶

◀

▶

Back

Close

Full Screen / Esc

Printer-friendly Version

Interactive Discussion



**WRF–ACASA
coupling**

L. Xu et al.

[Title Page](#)[Abstract](#)[Introduction](#)[Conclusions](#)[References](#)[Tables](#)[Figures](#)[◀](#)[▶](#)[◀](#)[▶](#)[Back](#)[Close](#)[Full Screen / Esc](#)[Printer-friendly Version](#)[Interactive Discussion](#)

land surface interaction with the atmosphere because it indicates conditions for con-
densation. The disparities between the WRF–ACASA and WRF–NOAH models are
more distinct in the dew point temperature than in the surface temperature. While both
models perform well with the surface temperature simulation, the WRF–ACASA model
outperforms the WRF–NOAH in simulating the dew point temperature especially over
the San Joaquin Station and during May for the Mojave Desert station. This could
be due to the complex physiological processes in the WRF–ACASA model that allow
a better simulation of the humidity profile and physiological interactions. Although the
vegetation covers over these two regions are sparse, the multilayer canopy structure in
the WRF–ACASA model is likely to retain moisture longer within the canopy. Therefore,
the dew point temperature from WRF–ACASA is better simulated than the WRF–NOAH
model, which is a single canopy layer model. However, both models have difficulty over
the Mojave Desert Station where they underestimated the dew point temperature as
much as 15 °C during February and November. Similar to the surface temperature anal-
ysis, both models performed best over the Northeast Plateau station with well-matched
land cover type and simple canopy structure of a short grass. In general, the dew point
temperature simulations from the WRF–ACASA model match closely with the obser-
vations in magnitude and timing.

Figure 11 presents diurnal patterns of surface dew point temperature for the four
different seasons. Unlike for the surface air temperature, there is relatively little diurnal
variation in the surface dew point temperature throughout the seasons and locations.
The simulated dew point temperatures in both WRF–ACASA and WRF–NOAH are
functions of surface pressure and surface water vapor mixing ratio. Since the surface
pressure does not change dramatically throughout the day, changes in dew point tem-
perature are mainly due to fluctuations in water vapor mixing ratio. Once again, the dry
arid and low vegetated Mojave Desert site is problematic for both WRF–ACASA and
WRF–NOAH models.

Figure 12 shows scatter plots of Compared to the surface temperature, Fig. 12 shows
that the model simulations on dew point temperature exhibit more scatter than for other

WRF–ACASA coupling

L. Xu et al.

Title Page

Abstract

Introduction

Conclusions

References

Tables

Figures

◀

▶

◀

▶

Back

Close

Full Screen / Esc

Printer-friendly Version

Interactive Discussion



observational sets examined thus far. Although Fig. 10 seems to indicate that for Mo-
jave Desert Station, WRF–ACASA has a better agreement with surface observations,
the seasonal patterns for the entire Mojave Desert Basin show that both WRF–ACASA
model and WRF–NOAH performances are comparatively poor in this sparsely vege-
tated region. The choice of land surface model did not affect the model simulation,
hence the problem could be in the atmospheric processes in WRF and not in the land
surface processes.

This could be the result of the assumption of horizontal homogeneity in each of the
8 km×8 km grid cell used in both WRF–ACASA and WRF–NOAH model. A single model
grid cell that is not representative of all stations could be representing several observa-
tion stations with different microclimatic conditions. This is especially important when
the shrublands in the Mojave Desert Basin have different degrees of canopy openness.
Surprisingly, unlike the pervious analysis, Fig. 12 shows that the WRF–ACASA model
underperforms relative to WRF–NOAH over the Northeast Plateau basin, with the cor-
relation between the model simulation and the observations lower than WRF–NOAH.

Figure 13 compares the relative humidity from both WRF–ACASA and WRF–NOAH
with the surface observation for four different locations during February, May, August
and October of 2005. Except for Mountain Counties station, both models fall mostly
within the 1 standard deviation range with the WRF–ACASA model showing some-
what better agreement than the WRF–NOAH model over the Mojave Desert Station.
The WRF–NOAH model underestimates the relative humidity for Mojave Desert and
San Joaquin Valley throughout the year. Although there is a land cover mismatch
between the actual station and the model, the higher relative humidity values in the
WRF–ACASA simulation compared with WRF–NOAH during the warm season rein-
force that the multi-layer canopy structure and higher order turbulent closure scheme
help the vegetation parameterization to simulate the retention of more moisture within
the canopy layers.

The land cover mismatch in the model could lead to overestimation of the relative
humidity in areas of low vegetation cover. The high LAI values over the Central Valley

WRF–ACASA
coupling

L. Xu et al.

[Title Page](#)[Abstract](#)[Introduction](#)[Conclusions](#)[References](#)[Tables](#)[Figures](#)[◀](#)[▶](#)[◀](#)[▶](#)[Back](#)[Close](#)[Full Screen / Esc](#)[Printer-friendly Version](#)[Interactive Discussion](#)

layer “big leaf” to represent the surface layer for all land cover types. In all single-layer models such as NOAH, there is no interaction and mixing within the canopy regardless of the specified vegetation type. As a result, the NOAH land surface model assumes that the entire canopy has similar physical and physiological properties as a single big leaf. In contrast, the ACASA land surface model uses a multi-layer canopy structure that varies according to different land cover type. The complex physically based model includes the intricate surface processes such as canopy structure, turbulent transport and mixing within and above the canopy and sublayers, and the interactions between the canopy elements and the surrounding air. Light and precipitation from the atmospheric layers above are intercepted, infiltrated, and reflect within the canopy layers and along with other meteorological and environmental forcings to drive plant physiological responses. In addition, the higher order closure scheme in the model allows both down- and counter-gradient transport of carbon dioxide, water vapor, heat, and momentum within and above the canopy layers and interact with the atmosphere. Through plant evapotranspiration, photosynthesis, respiration, and roughness length, the surface ecosystem transforms the environmental conditions and influences the atmosphere processes above such as modifications on surface temperature, dew point temperature, and relative humidity. Therefore, compared to the WRF–NOAH with simplified surface and ecosystem representation, the WRF–ACASA coupled model presents a detailed picture of the physical and physiological interactions between the land surface and the atmosphere. However, when compared to 2 m near surface observations, WRF–ACASA simulation output may have the qualification that it could be simulating understory microclimate, compared to WRF–NOAH’s big leaf with no understory, and the ARB stations that are usually over short grasses or bare surfaces.

The comparisons between model simulations and surface observations show that the WRF–ACASA model is able to soundly simulate surface and atmospheric conditions. Its simulation of temperature, dew point temperature, and relative humidity agree well with the surface observations overall. While overall both WRF–ACASA and WRF–NOAH simulations agree well with the surface observations, model performances vary

**WRF–ACASA
coupling**

L. Xu et al.

[Title Page](#)[Abstract](#)[Introduction](#)[Conclusions](#)[References](#)[Tables](#)[Figures](#)[◀](#)[▶](#)[◀](#)[▶](#)[Back](#)[Close](#)[Full Screen / Esc](#)[Printer-friendly Version](#)[Interactive Discussion](#)

between the two approaches of land surface representations depending on surface and atmosphere conditions. For example, during the cold and wet winter, surface temperature, dew point temperature and relative humidity from both models have high degree of agreement as well as high correlation with the surface observations. However, as the season starts to warm up, a temperature bias for WRF–ACASA in certain regions begin to increase. Maximum daytime temperatures in the WRF–ACASA simulations are systematically lower than the observed daily maximum during the warmer months over low vegetated regions such as the Mojave Desert. This temperature bias is likely due to the surface representation in the WRF–ACASA model producing too much evaporative cooling from high leaf area index. For the shrubland vegetation with low leaf area index, the leaf area indices for each of the sub-canopy layers are further reduced. The higher order turbulent closure scheme more effectively reflects the energy transport away from the surface level to induce heat loss. These thermodynamically processes in the WRF–ACASA model allow describing the prolonged period of cooling in early mornings. As a result, the high daytime temperature is underestimated in the multi-layer model.

The analysis of dew point temperature and relative humidity on the other hand shows that these more detailed physical processes in WRF–ACASA seem to improve the dew point temperature and relative humidity simulations compared to the WRF–NOAH model. The process parameterizations appear to allow the retention of more moisture within the canopy layers as well as the distribution of moisture within and above the canopy. Compared to the WRF–NOAH model, the WRF–ACASA model has a more complex and detailed canopy and plant physiological process parameterizations to more realistically represent the ecosystem-atmosphere interactions. The model simulations of the two models agree well with the surface observations through time and space as showed in temperature, dew point temperature and relative humidity.

Overall, when compared to the simple single layer WRF–NOAH model, the WRF–ACASA model has greater model complexity to present a more detailed picture of how the atmosphere and ecosystems interact including ecophysiological activities such as photosynthesis and respiration without decreasing the quality of the output. Finally,

this study describes the newly coupled WRF–ACASA model and its performance in simulating the surface conditions over the complex terrain and vegetated regions of California. The physical and physiological processes in the WRF–ACASA model highlight the effect of different land surface components and their overall impacts on atmospheric conditions. In addition, the WRF–ACASA model provides the opportunities to study more questions involving the ecosystem responses to the atmospheric impacts such as the contribution of irrigation on canopy energy distribution, land use transformations, climate change, and other dynamic and biosphere–atmospheric interactions.

Code availability

The source code of the WRF–ACASA can be obtained upon request. The code can be compiled and ran using platforms that support the WRF model. For code request, please contact Liyi Xu, liyixm@mit.edu.

Acknowledgements. This work is in part supported by the National Science Foundation under Awards No. ATM-0619139. The Joint Program on the Science and Policy of Global Change is funded by a number of federal agencies and a consortium of 40 industrial and foundation sponsors. (For the complete list see <http://globalchange.mit.edu/sponsors/current.html>.)

We also thank Matthias Falk for his inputs on the WRF–ACASA work.

References

- Borge, R., Alexandrov, V., José del Vas, J., Lumberras, J., and Rodríguez, E.: A comprehensive sensitivity analysis of the WRF model for air quality applications over the Iberian Peninsula, *Atmos. Environ.*, 42, 8560–8574, 2008. 2834
- Chen, F. and Avissar, R.: The impact of land-surface wetness heterogeneity on mesoscale heat fluxes, *J. Appl. Meteorol.*, 33, 1323–1340, 1994. 2831

GMDD

7, 2829–2875, 2014

WRF–ACASA coupling

L. Xu et al.

Title Page

Abstract

Introduction

Conclusions

References

Tables

Figures

◀

▶

◀

▶

Back

Close

Full Screen / Esc

Printer-friendly Version

Interactive Discussion



WRF–ACASA
coupling

L. Xu et al.

Title Page

Abstract

Introduction

Conclusions

References

Tables

Figures

◀

▶

◀

▶

Back

Close

Full Screen / Esc

Printer-friendly Version

Interactive Discussion



Chen, F. and Dudhia, J.: Coupling an advanced land surface–hydrology model with the Penn State-NCAR MM5 modeling system. Part I: Model implementation and sensitivity, *Mon. Weather Rev.*, 129, 569–585, 2001a. 2832

Chen, F. and Dudhia, J.: Coupling an advanced land surface–hydrology model with the Penn State-NCAR MM5 modeling system. Part II: Preliminary model validation, *Mon. Weather Rev.*, 129, 587–604, 2001b. 2832

Chen, S. H. and Dudhia, J.: Annual report: WRF physics, Air Force Weather Agency, 38 pp., 2000. 2833, 2834

Chen, S. and Sun, W.: A one-dimensional time dependent cloud model, *J. Meteorol. Soc. Jpn.*, 80, 99–118, 2002. 2839

Denmead, O. and Bradley, E.: Flux–gradient relationships in a forest canopy, in: *The Forest–Atmosphere Interaction: Proceedings of the Forest Environmental Measurements Conference*, edited by: Hutchison, B. and Hicks, B., D. Reidel Publishing Company, Oak Ridge, TN, 421–442, 1985. 2836

de Wit, M.: Modelling nutrient fluxes from source to river load: a macroscopic analysis applied to the Rhine and Elbe basins, *Hydrobiologia*, 410, 123–130, 1999. 2833

Dickinson, R., Henderson-Sellers, A., and Kennedy, P.: Biosphere–Atmosphere Transfer Scheme (BATS) Version 1e as coupled to the NCAR community model, NCAR Tech. Note NCAR/TN-387+ STR, 72, National Center for Atmospheric Research, Boulder, Colorado, 1993. 2834

Duan, Q., Sorooshian, S., and Gupta, V.: Effective and efficient global optimization for conceptual rainfall-runoff models, *Water Resour. Res.*, 28, 1015–1031, 1992. 2832

Dudhia, J.: Numerical study of convection observed during the winter monsoon experiment using a mesoscale two-dimensional model, *J. Atmos. Sci.*, 46, 3077–3107, 1989. 2839

Etchevers, P., Martin, E., Brown, R., Fierz, C., Lejeune, Y., Bazile, E., Boone, A., Dai, Y., Essery, R., Fernandez, A., Gusev, Y., Jordan, R., Koren, V., Kowalczyk, E., Nasonova, O. N., Pyles, R. D., Schlosser, A., Shmakin, A. B., Smirnova, T. G., Strasser, U., Versegny, D., Yamazaki, T., and Yang, Z.-L.: Validation of the energy budget of an alpine snowpack simulated by several snow models (SnowMIP project), *Ann. Glaciol.*, 38, 150–158, 2004. 2837

Gao, W., Shaw, R., and Paw U, K.: Observation of organized structure in turbulent flow within and above a forest canopy, *Bound.-Lay. Meteorol.*, 47, 349–377, 1989. 2836

WRF–ACASA
coupling

L. Xu et al.

Title Page

Abstract

Introduction

Conclusions

References

Tables

Figures

◀

▶

◀

▶

Back

Close

Full Screen / Esc

Printer-friendly Version

Interactive Discussion



Holtslag, A. and Ek, M.: Simulation of surface flux and boundary layer development over the pine forest in HAPEX-MOBILHY, *J. Appl. Meteorol.*, 35, 202–213, doi:10.1175/1520-0450(1996)035<0202:SOSFAB>2.0.CO;2, 1996. 2834

Hong, S. and Pan, H.: Nonlocal boundary layer vertical diffusion in a medium-range forecast model, *Mon. Weather Rev.*, 124, 2322–2339, 1996. 2839

Houborg, R. and Soegaard, H.: Regional simulation of ecosystem CO₂ and water vapor exchange for agricultural land using NOAA AVHRR and Terra MODIS satellite data. Application to Zealand, Denmark, *Remote Sens. Environ.*, 93, 150–167, 2004. 2832

Jarvis, P.: The interpretation of the variations in leaf water potential and stomatal conductance found in canopies in the field, *Philos. T. R. Soc. A*, 273, 593–610, 1976. 2832, 2834

Jetten, V., de Roo, A., and Favis-Mortlock, D.: Evaluation of field-scale and catchment-scale soil erosion models, *Catena*, 37, 521–541, 1999. 2833

Mahrt, L. and Ek, M.: The influence of atmospheric stability on potential evaporation, *J. Clim. Appl. Meteorol.*, 23, 222–234, 1984. 2834

Marras, S., Spano, D., Sirca, C., Duce, P., Snyder, R., Pyles, R., Paw U, K. T., and Tha, K.: Advanced-Canopy–Atmosphere–Soil Algorithm (ACASA model) for estimating mass and energy fluxes, *Ital. J. Agron.*, 3, 793–794, 2008. 2837

Marras, S., Pyles, R., Sirca, C., Paw U, K. T., Snyder, R., Duce, P., and Spano, D.: Evaluation of the Advanced Canopy–Atmosphere–Soil Algorithm (ACASA) model performance over Mediterranean maquis ecosystem, *Agr. Forest Meteorol.*, 151, 730–745, 2011. 2837

Meyers, T. and Paw U, K.: Testing of a higher-order closure model for modeling airflow within and above plant canopies, *Bound.-Lay. Meteorol.*, 37, 297–311, 1986. 2836

Meyers, T. and Paw U, K. T.: Modelling the plant canopy micrometeorology with higher-order closure principles, *Agr. Forest Meteorol.*, 41, 143–163, 1987. 2836

Miglietta, M. and Rotunno, R.: Simulations of moist nearly neutral flow over a ridge, *J. Atmos. Sci.*, 62, 1410–1427, 2005. 2834

Mintz, Y.: A brief review of the present status of global precipitation estimates, *Precipitation Measurements from Space-Workshop Report*, Atlas, D. and Thiele, O. W., NASA Goddard Space Flight Center, Greenbelt, MD, 1981. 2831

Mlawer, E., Taubman, S., Brown, P., Iacono, M., and Clough, S.: Radiative transfer for inhomogeneous atmospheres: RRTM, a validated correlated-*k* model for the longwave, *J. Geophys. Res.*, 102, 16663–16682, 1997. 2839

WRF–ACASA
coupling

L. Xu et al.

Title Page

Abstract

Introduction

Conclusions

References

Tables

Figures

◀

▶

◀

▶

Back

Close

Full Screen / Esc

Printer-friendly Version

Interactive Discussion



- Noilhan, J. and Planton, S.: A simple parameterization of land surface processes for meteorological models, *Mon. Weather Rev.*, 117, 536–549, 1989. 2834
- Paw U, K. T. and Gao, W.: Applications of solutions to non-linear energy budget equations, *Agr. Forest Meteorol.*, 43, 121–145, 1988.
- 5 Perrin, C., Michel, C., and Andréassian, V.: Does a large number of parameters enhance model performance? Comparative assessment of common catchment model structures on 429 catchments, *J. Hydrol.*, 242, 275–301, 2001. 2833
- Pielke, R., Marland, G., Betts, R., Chase, T., Eastman, J., Niles, J., Niyogi, S., and Running, S.: The influence of land-use change and landscape dynamics on the climate system: relevance to climate-change policy beyond the radiative effect of greenhouse gases, *Philos. T. R. Soc. A*, 360, 1705–1719, 2002. 2831
- 10 Pleim, J. and Xiu, A.: Development and testing of a surface flux and planetary boundary layer model for application in mesoscale models, *J. Appl. Meteorol.*, 34, 16–32, 1995. 2832
- Powers, J.: Numerical prediction of an Antarctic severe wind event with the Weather Research and Forecasting (WRF) model, *Mon. Weather Rev.*, 135, 3134–3157, 2007. 2834
- 15 Pyles, R., Weare, B., and Paw U, K. T.: The UCD Advanced Canopy–Atmosphere–Soil Algorithm: comparisons with observations from different climate and vegetation regimes, *Q. J. Roy. Meteor. Soc.*, 126, 2951–2980, 2000. 2837
- Pyles, R., Weare, B., Paw U, K. T., and Gustafson, W.: Coupling between the University of California, Davis, Advanced Canopy–Atmosphere–Soil Algorithm (ACASA) and MM5: preliminary results for July 1998 for western North America, *J. Appl. Meteorol.*, 42, 557–569, 2003. 2840
- 20 Pyles, R., Paw U, K. T., and Falk, M.: Directional wind shear within an old-growth temperate rainforest: observations and model results, *Agr. Forest Meteorol.*, 125, 19–31, 2004. 2831, 2837
- 25 Raupach, M. and Finnigan, J.: Single-layer models of evaporation from plant canopies are incorrect but useful, whereas multilayer models are correct but useless: discuss, *Aust. J. Plant Physiol.*, 15, 705–716, 1988. 2833
- Rowntree, P.: Atmospheric parameterization schemes for evaporation over land: basic concepts and climate modeling aspects, in: *Land Surface Evaporation: Measurement and Parameterization*, edited by: Schmugge, T. and André, J.-C., Springer-Verlag, New York, 5–29, 1991. 2831
- 30

WRF–ACASA
coupling

L. Xu et al.

Title Page

Abstract

Introduction

Conclusions

References

Tables

Figures

◀

▶

◀

▶

Back

Close

Full Screen / Esc

Printer-friendly Version

Interactive Discussion



- Rutter, N., Essery, R., Pomeroy, J., Altimir, N., Andreadis, K., Baker, I., Barr, A., Bartlett, P., Boone, A., Deng, H., Douville, H., Dutra, E., Elder, K., Ellis, C., Feng, X., Gelfan, A., Goodbody, A., Gusev, Y., Gustafsson, D., Hellstrom, R., Hirabayashi, Y., Hirota, T., Jonas, T., Koren, V., Kuragina, A., Lettenmaier, D., Li, W.-P., Luce, C., Martin, E., Nasanova, O., Pumpanen, J., Pyles, R., Samuelsson, P., Sandells, M., Schädler, G., Shmakin, A., Smirnova, T., Stähli, M., Stöckli, R., Strasser, U., Su, H., Suzuki, K., Takata, K., Tanaka, K., Thompson, E., Vesala, T., Viterbo, P., Wiltshire, A., Xia, K., Xue, Y., and Yamazaki, T.: Evaluation of forest snow process models (SnowMip2), *J. Geophys. Res.*, 114, D06111, doi:10.1029/2008JD011063, 2009. 2837
- 5 Sellers, P., Tucker, C., Collatz, G., Los, S., Justice, C., Dazlich, D., and Randall, D.: A revised land surface parameterization (SiB2) for atmospheric GCMs. Part II: The generation of global fields of terrestrial biophysical parameters from satellite data, *J. Climate*, 9, 706–737, 1996. 2834
- 10 Smirnova, T., Brown, J., and Benjamin, S.: Performance of different soil model configurations in simulating ground surface temperature and surface fluxes, *Mon. Weather Rev.*, 125, 1870–1884, 1997. 2832
- 15 Smirnova, T., Brown, J., Benjamin, S., and Kim, D.: Parameterization of cold-season processes in the MAPS, *J. Geophys. Res.*, 105, 4077–4086, 2000. 2832
- 20 Staudt, K., Serafimovich, A., Siebicke, L., Pyles, R., and Falge, E.: Vertical structure of evapotranspiration at a forest site (a case study), *Agr. Forest Meteorol.*, 151, 709–729, 2011. 2837
- Stauffer, D. and Seaman, N.: Use of four-dimensional data assimilation in a limited-area mesoscale model. Part I: Experiments with synoptic-scale data, *Mon. Weather Rev.*, 118, 1250–1277, 1990. 2839
- 25 Stauffer, D., Seaman, N., and Binkowski, F.: Use of four-dimensional data assimilation in a limited-area mesoscale model. II – Effects of data assimilation within the planetary boundary layer, *Mon. Weather Rev.*, 119, 734–754, 1991. 2839
- Stull, R. B.: *An Introduction to Boundary Layer Meteorology*, Kluwer Academic Publishers, Dordrecht, 1988. 2831, 2844
- 30 Su, H., Paw U, K. T., and Shaw, R.: Development of a coupled leaf and canopy model for the simulation of plant–atmosphere interactions, *J. Appl. Meteorol.*, 35, 733–748, 1996. 2836
- Thompson, S., Govindasamy, B., Mirin, A., Caldeira, K., Delire, C., Milovich, J., Wickett, M., and Erickson, D.: Quantifying the effects of CO₂-fertilized vegetation on future global climate

and carbon dynamics, *Geophys. Res. Lett.*, 31, L23211, doi:10.1029/2004GL021239, 2004. 2834

Trenberth, K. and Shea, D.: Atlantic hurricanes and natural variability in 2005, *Geophys. Res. Lett.*, 33, L12704, doi:10.1029/2006GL026894, 2006. 2834

5 Wieringa, J.: Roughness-dependent geographical interpolation of surface wind speed averages, *Q. J. Roy. Meteor. Soc.*, 112, 867–889, 1986. 2831

Xiu, A. and Pleim, J.: Development of a land surface model. Part I: Application in a mesoscale meteorological model, *J. Appl. Meteorol.*, 40, 192–209, 2001. 2832

10 Zhan, X. and Kustas, W.: A coupled model of land surface CO₂ and energy fluxes using remote sensing data, *Agr. Forest Meteorol.*, 107, 131–152, 2001. 2832

Zhao, M., Pitman, A., and Chase, T.: The impact of land cover change on the atmospheric circulation, *Clim. Dynam.*, 17, 467–477, 2001. 2831

**WRF–ACASA
coupling**

L. Xu et al.

Title Page

Abstract

Introduction

Conclusions

References

Tables

Figures

◀

▶

◀

▶

Back

Close

Full Screen / Esc

Printer-friendly Version

Interactive Discussion



Table 2. Selected sites from the Air Resources Board meteorological stations network.

Season	Basin	R^2		RMSE		Degree of Agreement	
		WRF-NOAH	WRF-ACASA	WRF-NOAH	WRF-ACASA	WRF-NOAH	WRF-ACASA
DJF	SCC	0.831671	0.716923	1.73878	2.46986	0.91687	0.821745
MAM	SCC	0.98397	0.806324	1.32221	2.09018	0.987497	0.910685
JJA	SCC	0.603668	0.532604	2.03934	2.2107	0.93101	0.899527
SON	SCC	0.817867	0.8446	1.79367	1.7037	0.934533	0.951894
DJF	SJV	0.996713	0.944033	1.49348	1.55048	0.996796	0.969605
MAM	SJV	0.989379	0.983285	1.81218	1.70317	0.991555	0.991714
JJA	SJV	0.981085	0.790353	2.24522	2.77545	0.97525	0.71053
SON	SJV	0.995999	0.836214	1.9562	2.83981	0.997329	0.88651
DJF	NCC	0.738797	0.624952	1.4336	2.15347	0.885708	0.703579
MAM	NCC	0.977027	0.804917	1.21572	1.65924	0.98831	0.952791
JJA	NCC	0.891338	0.796365	1.91748	1.78896	0.968166	0.947152
SON	NCC	0.945243	0.961512	1.53172	1.16758	0.96535	0.986446
DJF	SC	0.967272	0.913497	1.88247	1.64677	0.966178	0.948648
MAM	SC	0.993072	0.981621	1.55349	1.37131	0.993048	0.990378
JJA	SC	0.588722	0.580935	2.06404	3.4954	0.831568	0.595515
SON	SC	0.980249	0.710668	1.89105	2.40559	0.988638	0.831628
DJF	SV	0.986383	0.925806	1.1287	1.28074	0.991035	0.964948
MAM	SV	0.980696	0.981402	1.29392	1.21403	0.98801	0.992255
JJA	SV	0.997783	0.752783	1.64352	2.453	0.997999	0.67696
SON	SV	0.997573	0.881367	1.46927	2.09812	0.99837	0.919228
DJF	SD	0.951017	0.764242	1.46921	1.9857	0.96677	0.85756
MAM	SD	0.966413	0.926948	1.15405	1.26534	0.975935	0.973743
JJA	SD	0.487301	0.554737	2.05678	3.64936	0.768834	0.612857
SON	SD	0.875988	0.564617	1.47285	2.1236	0.946929	0.800983
DJF	GBV	0.813173	0.754106	2.7741	3.40534	0.952817	0.908663
MAM	GBV	0.93591	0.936978	2.36249	2.20798	0.962156	0.969805
JJA	GBV	0.853203	0.804406	2.84441	3.01706	0.856085	0.739935
SON	GBV	0.92474	0.917856	2.2518	2.34017	0.966767	0.963998
DJF	SFB	0.185791	0.284025	1.77587	2.0497	0.876986	0.886728
MAM	SFB	0.913346	0.63263	1.51517	2.0793	0.976113	0.941796
JJA	SFB	0.743593	0.495629	1.93917	3.10351	0.924286	0.768198
SON	SFB	0.950796	0.629486	1.4078	1.98632	0.981719	0.848947
DJF	SS	0.496889	0.727061	1.86463	2.19616	0.876449	0.901978
MAM	SS	0.994308	0.910398	1.2895	1.67741	0.996386	0.964686
JJA	SS	0.679887	0.391227	2.58393	2.63565	0.790626	0.684046
SON	SS	0.991819	0.769102	1.59417	3.04378	0.996416	0.865084
DJF	NEP	0.813234	0.762997	1.46407	1.81746	0.947417	0.897551
MAM	NEP	0.926788	0.928542	2.14003	1.96821	0.968855	0.976753
JJA	NEP	0.743007	0.59725	2.09303	2.52024	0.861164	0.769247
SON	NEP	0.987654	0.936724	1.54218	1.83687	0.99447	0.972525
DJF	MD	0.991988	0.904003	1.37581	1.27348	0.996475	0.971514
MAM	MD	0.969527	0.921582	1.62038	1.88437	0.982023	0.969443
JJA	MD	0.957873	0.74645	1.99593	2.84406	0.960473	0.72887
SON	MD	0.948833	0.824341	1.90569	2.55955	0.966272	0.884061
DJF	MC	0.983341	0.945083	1.61558	1.75623	0.982671	0.952361
MAM	MC	0.965586	0.991983	1.87782	1.76668	0.977757	0.996098
JJA	MC	0.898993	0.830306	2.1299	2.39603	0.893741	0.834615
SON	MC	0.982515	0.963089	1.81802	1.81886	0.987068	0.977584
DJF	NC	0.890632	0.751115	1.45055	1.89727	0.96326	0.919472
MAM	NC	0.677484	0.64897	3.47913	3.17359	0.872094	0.911504
JJA	NC	0.631845	0.631316	2.60202	2.92231	0.7467	0.629611
SON	NC	0.948986	0.876387	1.76809	1.87418	0.976128	0.951667

**WRF-ACASA
coupling**

L. Xu et al.

Title Page

Abstract

Introduction

Conclusions

References

Tables

Figures

⏪

⏩

◀

▶

Back

Close

Full Screen / Esc

Printer-friendly Version

Interactive Discussion



**WRF–ACASA
coupling**

L. Xu et al.

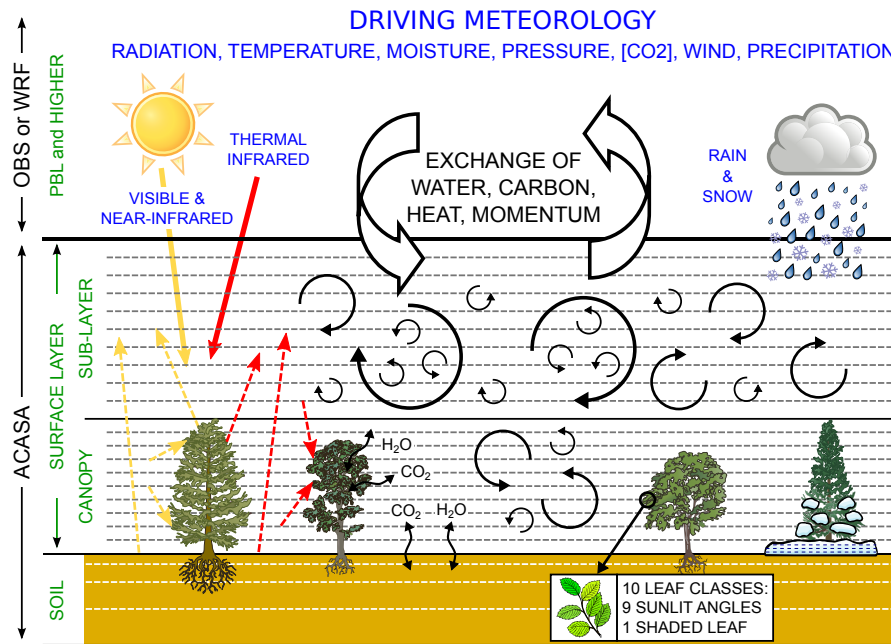


Fig. 1. The schematic diagram of the WRF–ACASA coupling.

[Title Page](#)

[Abstract](#) | [Introduction](#)

[Conclusions](#) | [References](#)

[Tables](#) | [Figures](#)

[◀](#) | [▶](#)

[◀](#) | [▶](#)

[Back](#) | [Close](#)

[Full Screen / Esc](#)

[Printer-friendly Version](#)

[Interactive Discussion](#)



WRF-ACASA
coupling

L. Xu et al.

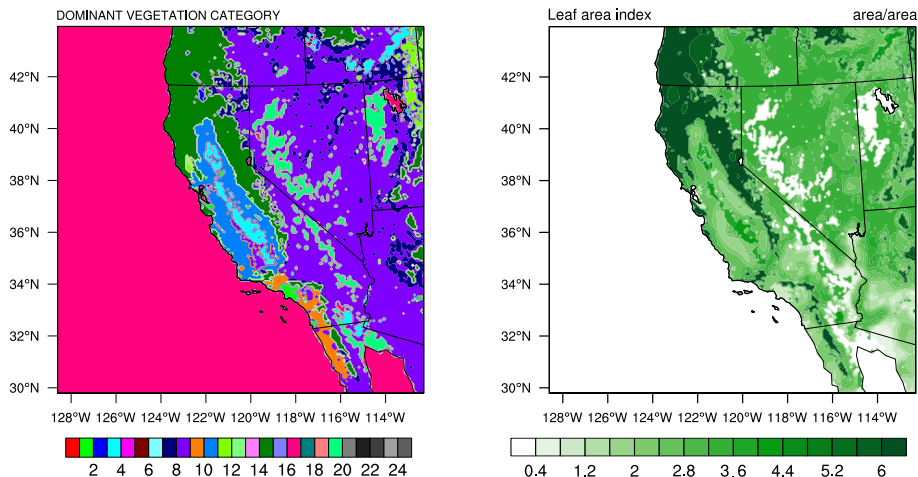


Fig. 2. The complex topography and land cover of the study domain is represented here by: (left) dominant vegetation type and (right) Leaf Area Index (LAI) from USGS used by the WRF model. The horizontal grid spacing of 8 km is needed to resolve the major topographical and ecological features of the domain.

[Title Page](#)[Abstract](#)[Introduction](#)[Conclusions](#)[References](#)[Tables](#)[Figures](#)[◀](#)[▶](#)[◀](#)[▶](#)[Back](#)[Close](#)[Full Screen / Esc](#)[Printer-friendly Version](#)[Interactive Discussion](#)

Map of ARB Surface Stations

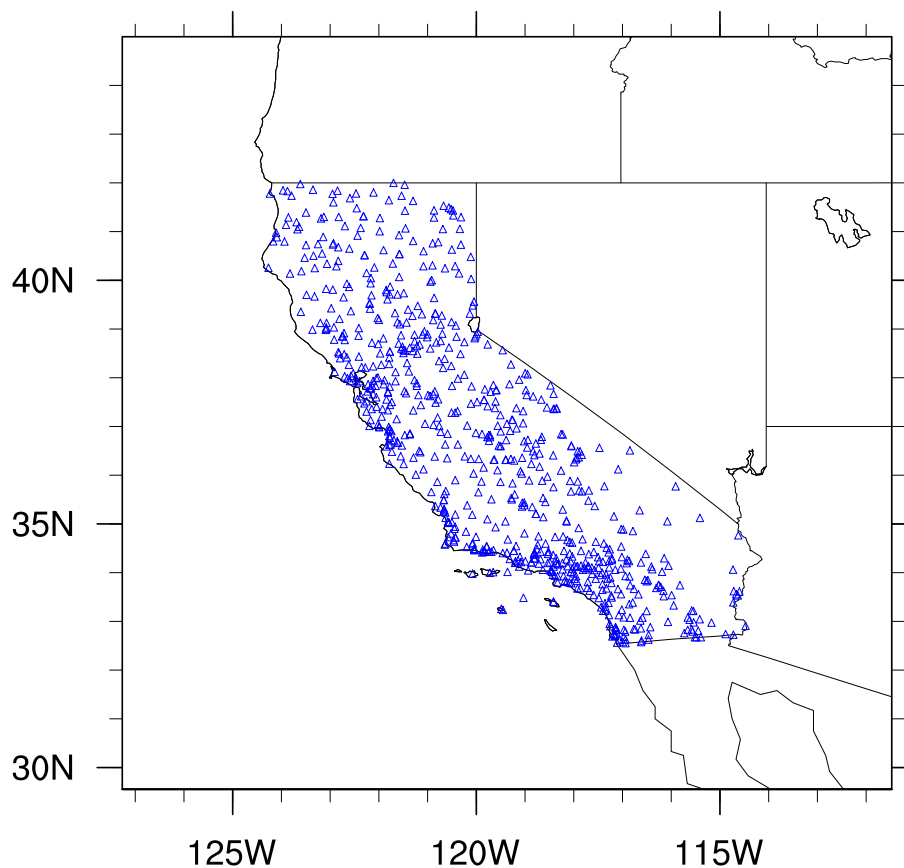


Fig. 3. Map of the location of the California Air Resources Board's surface stations.

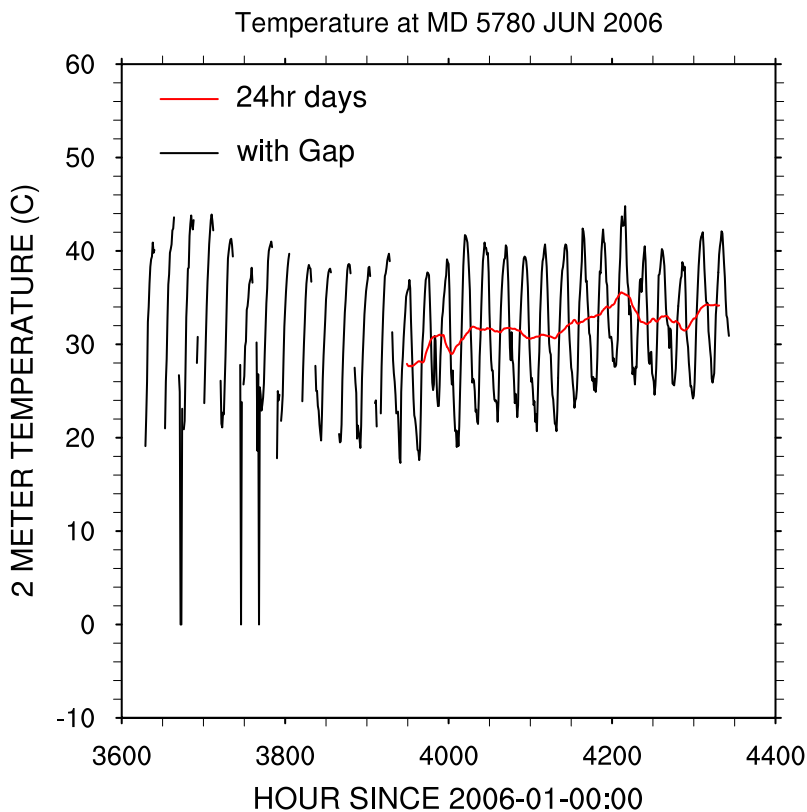


Fig. 4. Time series of the surface air temperature at Mojave Desert Station during June 2006. The black line represents the entire set of surface temperature observation with gaps presented. The red line represent the daily mean temperature calculated using only days with all 24 h of observation available.

**WRF-ACASA
coupling**

L. Xu et al.

Title Page

Abstract Introduction

Conclusions References

Tables Figures

◀ ▶

◀ ▶

Back Close

Full Screen / Esc

Printer-friendly Version

Interactive Discussion



Title Page

Abstract

Introduction

Conclusions

References

Tables

Figures

◀

▶

◀

▶

Back

Close

Full Screen / Esc

Printer-friendly Version

Interactive Discussion

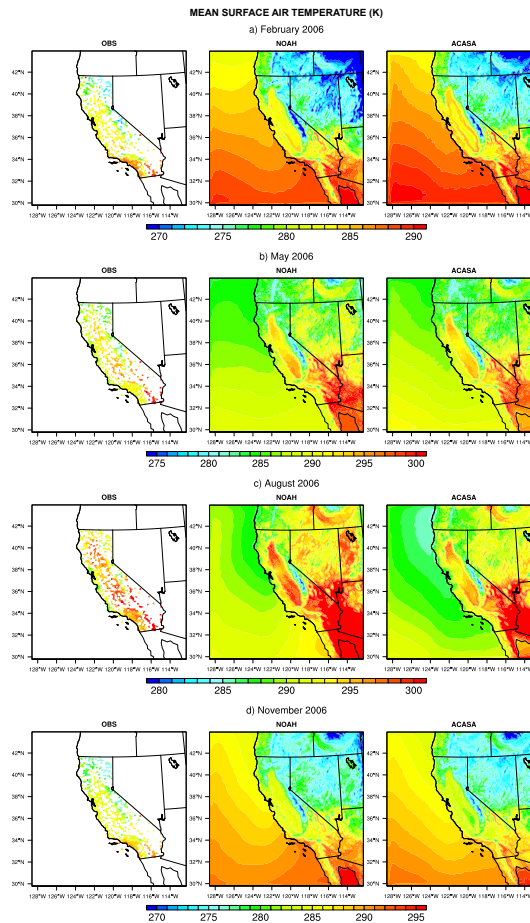


Fig. 5. Monthly mean surface air temperature simulated by WRF–ACASA and WRF–NOAH and for the surface observations for the months of February, May, August and November 2006.

**WRF–ACASA
coupling**

L. Xu et al.

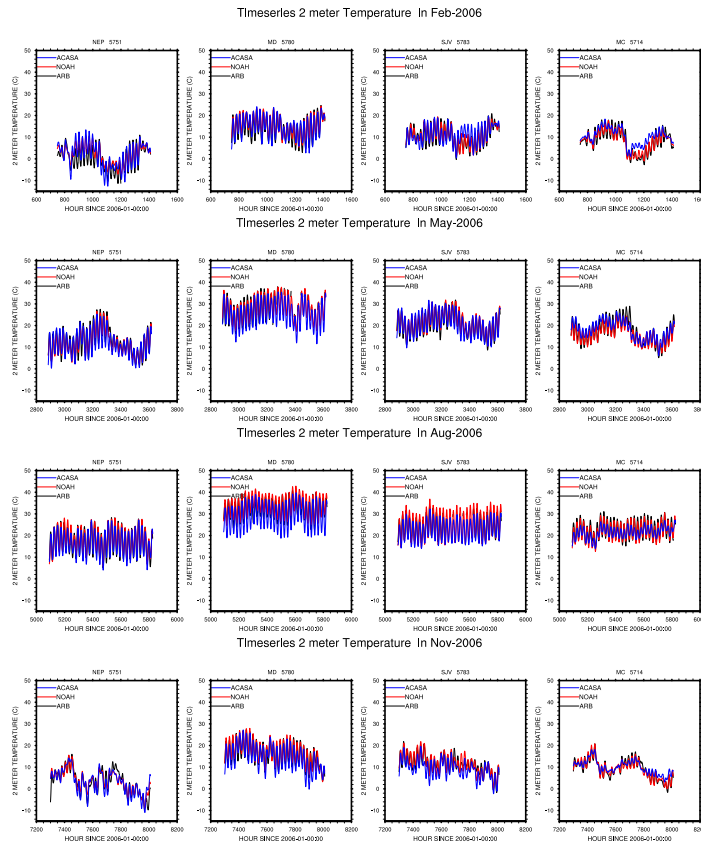


Fig. 6. Time series of surface air temperature simulated by WRF–ACASA and WRF–NOAH and for the surface observations for four different stations and for the months of February, May, August and November 2006.

[Title Page](#)
[Abstract](#) [Introduction](#)
[Conclusions](#) [References](#)
[Tables](#) [Figures](#)
⏪ ⏩
◀ ▶
[Back](#) [Close](#)
[Full Screen / Esc](#)
[Printer-friendly Version](#)
[Interactive Discussion](#)



WRF–ACASA
coupling

L. Xu et al.

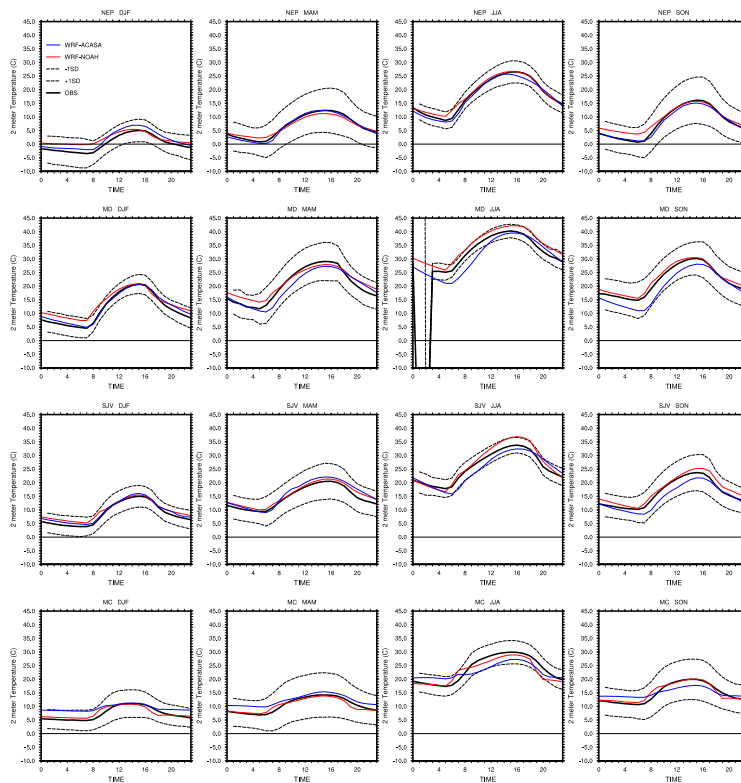


Fig. 7. Diurnal cycle of surface air temperature for each seasons for the Northeast Plateau, Mojave Desert, San Joaquin Valley, and Mountain County stations. The solid and the two dash black lines represent the surface observation and ± 1 standard deviation from the mean respectively. The WRF–ACASA results are showed in blue and the WRF–NOAH results are in red.

Title Page

Abstract

Introduction

Conclusions

References

Tables

Figures

◀

▶

◀

▶

Back

Close

Full Screen / Esc

Printer-friendly Version

Interactive Discussion



WRF–ACASA
coupling

L. Xu et al.

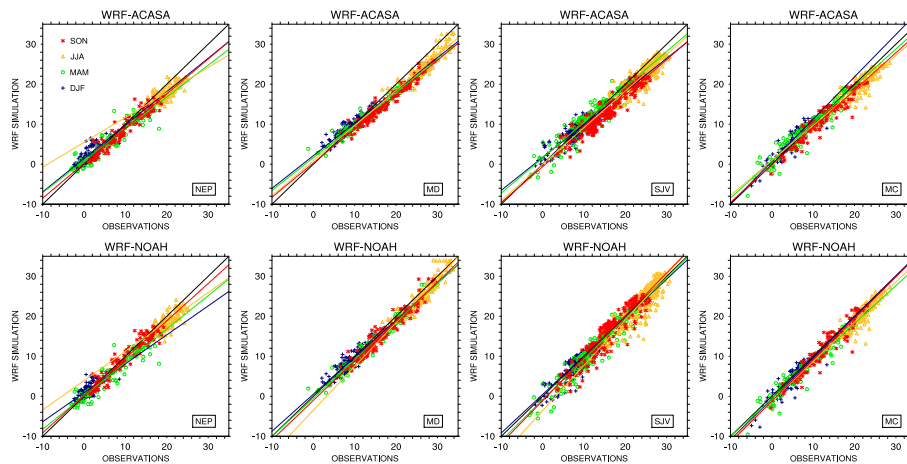


Fig. 8. Time series of surface air temperature simulated by WRF–ACASA and WRF–NOAH and for the surface observations for four different stations and for the months of February, May, August and November 2006.

Title Page

Abstract

Introduction

Conclusions

References

Tables

Figures

◀

▶

◀

▶

Back

Close

Full Screen / Esc

Printer-friendly Version

Interactive Discussion





Fig. 9. Statistical analysis of two model simulations vs. observed for *R*-square, Root Mean Square Error (RMSE), and Degree of Agreement for the four different seasons.

Title Page

Abstract

Introduction

Conclusions

References

Tables

Figures

⏪

⏩

◀

▶

Back

Close

Full Screen / Esc

Printer-friendly Version

Interactive Discussion



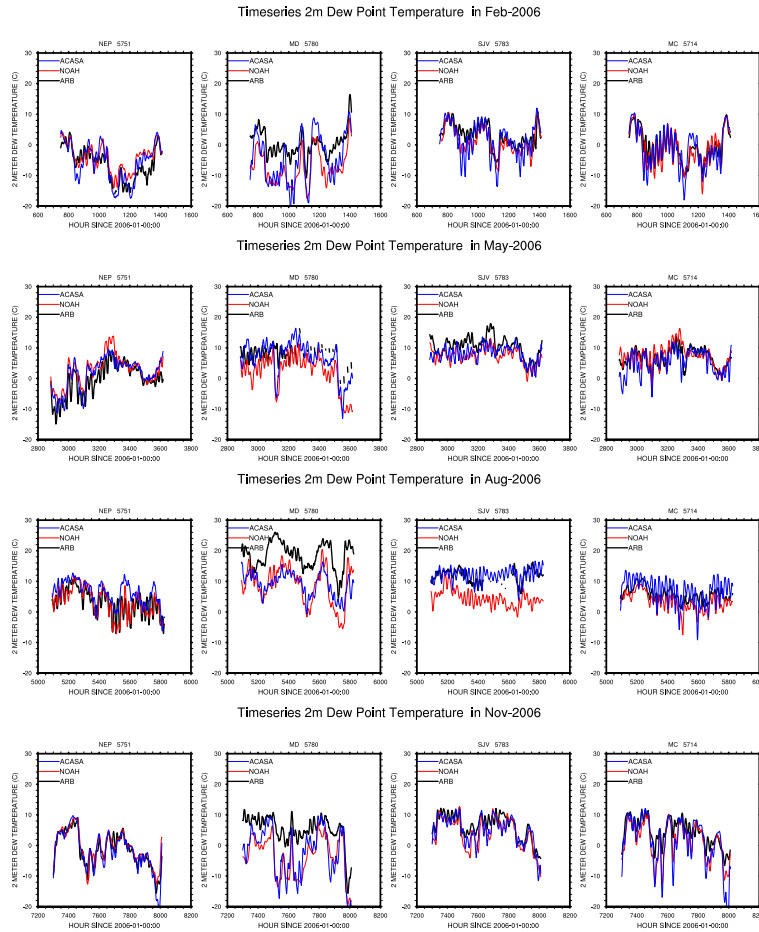


Fig. 10. Time series of dew point model predictions and observations for four basins during February, May, August, and November.

[Title Page](#)

[Abstract](#) [Introduction](#)

[Conclusions](#) [References](#)

[Tables](#) [Figures](#)

[⏪](#) [⏩](#)

[◀](#) [▶](#)

[Back](#) [Close](#)

[Full Screen / Esc](#)

[Printer-friendly Version](#)

[Interactive Discussion](#)



WRF-ACASA coupling

L. Xu et al.

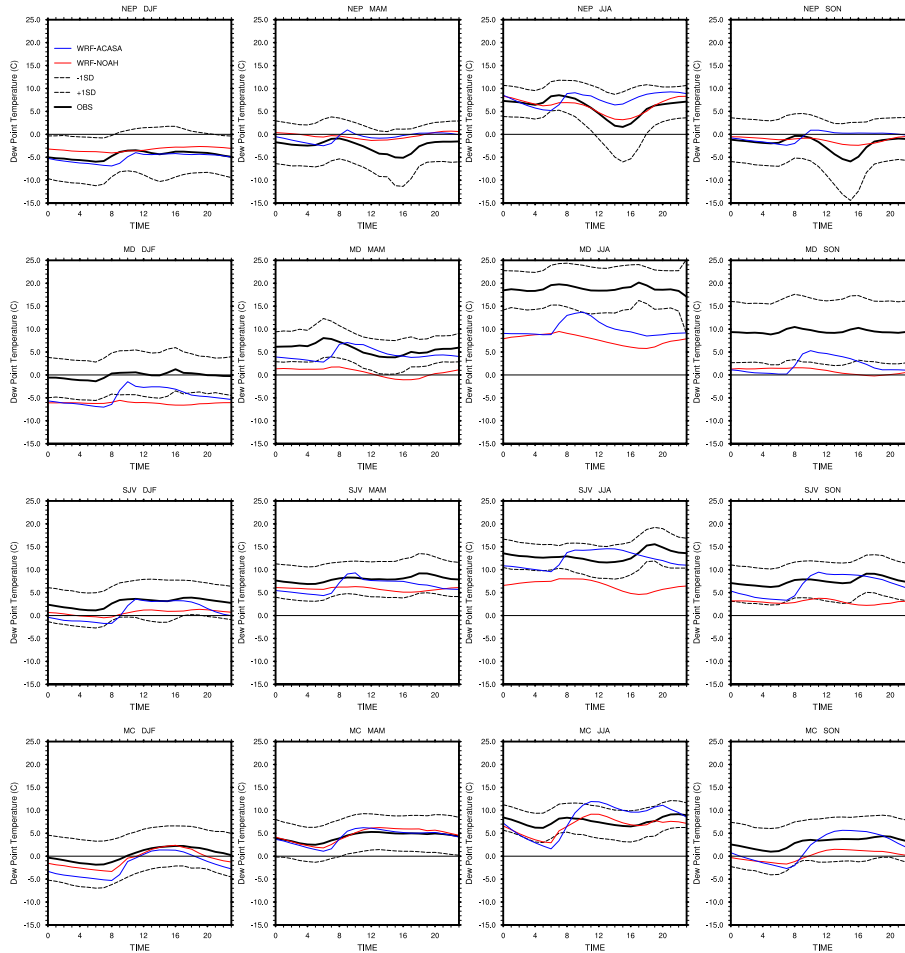


Fig. 11. Mean diurnal dew point temperature trends for the four seasons and the four air basins: northeast Plateau, Mojave Desert, San Joaquin Valley, and Mountain County stations.

Title Page

Abstract Introduction

Conclusions References

Tables Figures

⏪ ⏩

◀ ▶

Back Close

Full Screen / Esc

Printer-friendly Version

Interactive Discussion



WRF-ACASA
coupling

L. Xu et al.

Title Page

Abstract

Introduction

Conclusions

References

Tables

Figures

◀

▶

◀

▶

Back

Close

Full Screen / Esc

Printer-friendly Version

Interactive Discussion

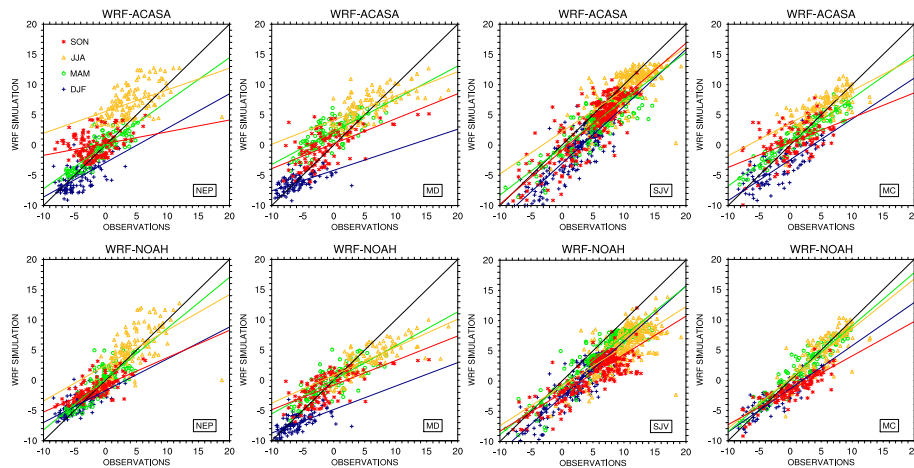


Fig. 12. Same as Fig. 8 but for surface dew point temperature.

**WRF–ACASA
coupling**

L. Xu et al.

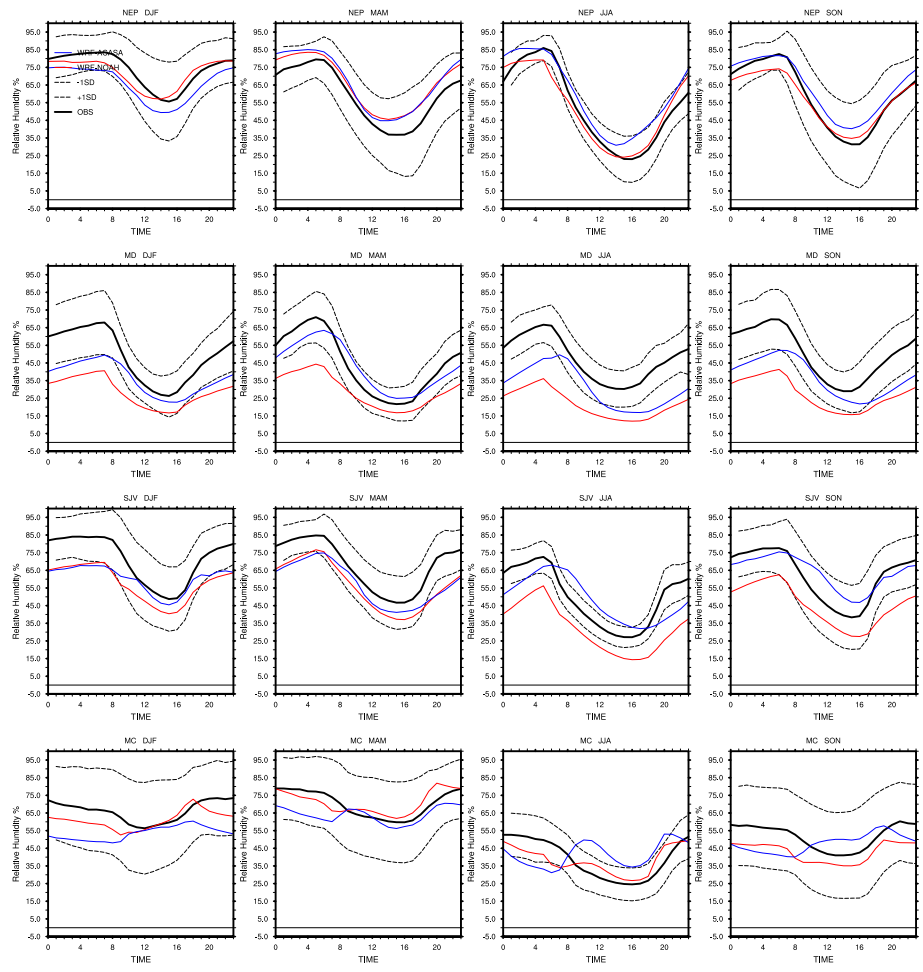


Fig. 13. Same as Fig. 8 but for surface relative humidity.

[Title Page](#)

[Abstract](#) [Introduction](#)

[Conclusions](#) [References](#)

[Tables](#) [Figures](#)

[⏪](#) [⏩](#)

[◀](#) [▶](#)

[Back](#) [Close](#)

[Full Screen / Esc](#)

[Printer-friendly Version](#)

[Interactive Discussion](#)



WRF–ACASA
coupling

L. Xu et al.

Title Page

Abstract

Introduction

Conclusions

References

Tables

Figures

◀

▶

◀

▶

Back

Close

Full Screen / Esc

Printer-friendly Version

Interactive Discussion

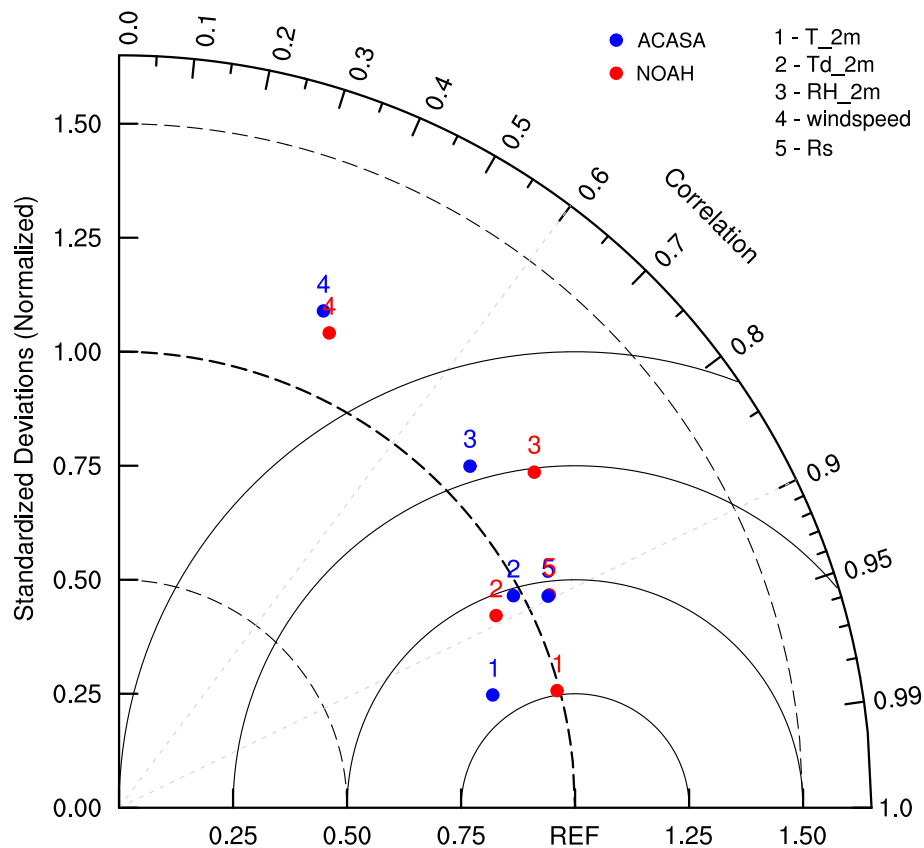


Fig. 14. Taylor diagram of monthly mean surface air temperature, dew point temperature, relative humidity, wind speed, and solar radiation for both WRF–ACASA and WRF–NOAH for all ARB stations. WRF–ACASA is represented by blue dots and WRF–NOAH by red dots.